Fluctuation Effects in the Complex Impedance of Superconducting Tin-Whisker Crystals near T_c†

John R. Miller* and John M. Pierce‡
Physics Department, University of Virginia, Charlottesville, Virginia 22901
(Received 2 April 1973)

An extensive experimental study of fluctuation effects in the complex ac impedance $Z_W(\omega,T)$ of one-dimensional tin-whisker crystals near the superconducting transition temperature T_c is described. The behavior of $Z_W(\omega,T)$ in ⟨001⟩ whiskers with cross-sectional areas 2×10^{-10}–3×10^{-9} cm^2 was measured at 60 MHz, 1 kHz, and dc from below T_c in the mean-field temperature range up through T_c and slightly above. Paraconductivity data were not obtained. By correlating high-frequency reactance data with resistance data from dc or low-frequency ac measurements, a more stringent test was made of the theory of fluctuation effects than is possible with dc measurements alone. We find that the theory of Langer and Ambegaokar (LA) as completed by McCumber and Halperin (MH) for the onset of resistance is inconsistent with our results unless the LA barrier height is reduced by a factor of approximately 0.55. If this is done, the LA-MH prediction agrees with resistance data over the full whisker size range. The MH result for the onset of fluctuation effects in the reactance agrees with our data without modification. No theory exists which can explain the behavior of $Z_W(\omega,T)$ as T passes through T_c. Our data are presented in a form to facilitate comparison with future theories. Reactance data in the mean-field region yield a direct measurement of the penetration depth. We find an interesting size effect in this quantity, and a new value is reported for the London penetration depth in pure tin, $\lambda_L = 289 \pm 20$ Å.

I. INTRODUCTION

The study of thermodynamic fluctuations in superconductors has received a great deal of experimental and theoretical effort in the past few years. The interplay between theory and experiment has brought deeper understanding of the dynamics of the electron system as it orders itself into the superconducting state. External manifestations of these fluctuations in bulk samples of superconductors are too small to observe, except above T_c. However, they can be studied, both above and below T_c, in samples that have one or more dimension reduced in size. In a wire with two dimensions smaller than the coherence length and penetration depth of the superconductor from which it is made, resistance due to fluctuations is observed well below T_c. The dc resistance of these "one-dimensional" superconductors has been extensively studied.[1–9] In this paper we report the results of the first extensive experimental study of the complex ac impedance of one-dimensional superconducting wires in a temperature range starting well below T_c and extending slightly above.[10]

Tin-whisker crystals are almost ideal one-dimensional samples to study. They can be grown quite small in diameter, and they are single crystals with few if any dislocations. Thus, they are quite strong and elastic for their size, a fact which has allowed us to handle and make measurements on whiskers down to ~1500 Å in diameter. Mean-free paths indicated by residual resistance ratios in these whiskers can be quite long relative to the coherence length. Thus they are "clean" in that sense. We have, however, observed interesting size effects in the penetration depth which indicate shorter effective mean-free paths for the superconductivity than are indicated by the residual resistance.

Measurements of the complex impedance at finite frequencies can detect the inertial reactance of the superconducting pairs, the so-called kinetic inductance. In the mean-field temperature range below T_c, this inductance is a direct measure of the pair density or penetration depth. We have used this fact to measure the size effects mentioned above and to extract a new value of the London penetration depth for Sn, $\lambda_L = 289 \pm 20$ Å. The behavior of the inductance in this temperature range also provides a value for the mean-field transition temperature T_c of the particular whisker, which is accurate to ~0.1 mK. This is extremely useful in comparing the fluctuation effects observed at higher temperatures with theory. As the temperature is increased, the first fluctuation effects appear in the reactance as a suppression of the pair density below its mean field value. Only at higher temperatures does significant fluctuation resistance appear. In order to produce resistance below T_c, the order parameter must undergo a drastic contortion from its equilibrium configuration, and these large fluctuations are quite rare until the immediate vicinity of T_c. This onset of resistance however, is the first indication of fluctuations which is accessible to a dc measurement. As the temperature increases above T_c, there is

a region of "paraconductivity" as the resistance approaches the normal resistance R_N, and the reactance approaches the ordinary magnetic reactance of a wire. Our data are unfortunately not reliable much above T_c, and we do not consider this paraconductivity here.[11]

We measure the impedance of each whisker as a function of temperature at three frequencies: 60 MHz, 1 kHz, and dc. By correlating data obtained at these three frequencies, it is possible to make a more stringent test of a theory relating to the fluctuation resistance than is possible with dc measurements alone. The ability to fix T_c accurately is an example of this. We find discrepancies between our measurements of the onset of resistance and the theory of Langer and Ambegaokar[12] (LA) as completed by McCumber and Halperin[13] (MH), which in the past appeared satisfactory on the basis of dc data alone.[6,7] The calculation of MH, however, does agree with our data for the initial suppression of the order parameter below the mean-field value before resistance appears. This fact has led us to question the LA result for the free-energy barrier height over which the system must pass during a resistance-producing fluctuation. By reducing the barrier height in the LA-MH theory by a simple factor of 0.55, we can fit our results for the onset of resistance in whiskers covering a large range of cross-sectional area $2.4-25\times10^{-10}$ cm^2.

No theories are available as yet which can explain quantitatively the variation of the full complex impedance as T passes through T_c. We do find, however, a qualitative correspondence between the observed reactance and recent calculations[14,15] of the average pair density $\langle|\psi|^2\rangle$. We simply present our data in the hope of stimulating further theoretical effort.

This paper is organized in four main sections. Section II contains a description of the equivalent circuit models we use to discuss the impedance of whiskers and an outline of the available theoretical calculations which are relevant to our results. Section III is a description of our experimental techniques and data-reduction methods, and the detailed results are presented in Sec. IV, which is divided in three parts. These cover mean-field properties, 60-MHz impedance results, and low-frequency resistance measurements, respectively. Preliminary reports of some of these results have appeared previously.[16-18]

II. THEORETICAL BACKGROUND

In order to provide a context in which to discuss our measurements of the ac impedance $Z_w(\omega, T)$ of tin-whisker crystals, we discuss here the equivalent circuit models we use to present the results and the theories which are relevant to them. Since our measurements are reliable only below T_c and slightly above, we concentrate primarily on the approach to T_c from lower temperatures.

As T is raised toward T_c in tin, a point is reached where the penetration depth $\lambda(T)$ becomes comparable to the temperature independent coherence length ξ_0. Above this point, the electrodynamics becomes local; there is a high density of quasiparticles which is nearly temperature independent and equal to the normal-state value; and the pair density $\langle|\psi|^2\rangle$ is low and decreasing toward zero. There is then a reasonably wide temperature range in which thermodynamic fluctuations are not important, and the mean field, Ginzburg-Landau picture of the superconductor is valid. In this model, $\langle|\psi|^2\rangle$ decreases linearly to zero at T_c. Our measurements begin in this mean-field region and extend up through the fluctuation region around T_c, where the mean-field theory breaks down. However, even in the fluctuation region, a two-fluid picture of a superconductor is still useful for discussing the impedance of a superconducting wire. There are resistive normal carriers in parallel with superconducting ones, which are essentially inductive. This picture is represented in Fig. 1.

We specialize now to wires which are small in radius compared with $\lambda(T)$. This ensures that the supercurrent is uniform across a wire and means that it is effectively one dimensional. Our whiskers meet this criterion over most of our temperature range. The circuit of Fig. 1(a) is a model for a one-dimensional whisker in the mean-field region.

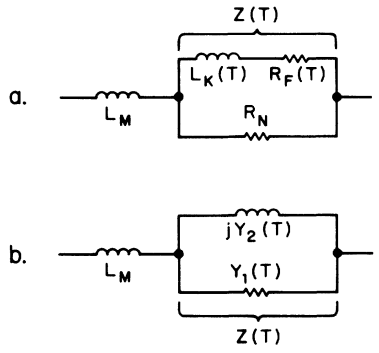

FIG. 1. Equivalent circuit representations for a one-dimensional superconductor near T_c. In both circuits, L_M is the magnetic inductance of the wire. A two-fluid model is represented by (a), in which the kinetic inductance L_K and fluctuation resistance R_F both become infinite above T_c, while the normal resistance R_N remains constant. A conductivity representation is shown in (b), where Y_1 and Y_2 are the real and imaginary parts of $1/Z(T)$. Thus, they are both temperature dependent. Above T_c, $Y_2 \to 0$, while $Y_1 \to R_N^{-1}$ both above and below T_c. Either circuit can represent an arbitrary $Z(T)$ function.

The quasiparticles contribute a resistance R_N which is temperature independent and equal to the normal-state resistance, while the pairs contribute an inductance L_K in parallel. A resistance R_F due to fluctuations appears near T_c in this channel as well. All the current flows through the ordinary magnetic inductance L_M. The kinetic inductance L_K, first discussed in this context by Little,[19] arises because the pair density is low enough that the kinetic energy of the pairs is significant. Its value in mks units is

$$L_K = m_e l/2e^2\langle|\psi|^2\rangle\sigma = \mu_0\lambda^2 l/\sigma\ , \tag{1}$$

where m_e and e are the electronic mass and charge and l and σ are the length and cross-sectional area of the whisker, respectively. Thus, a measurement of L_K in the mean-field region gives a direct measure of the pair density or penetration depth. At higher temperatures, where R_F is significant and ψ may fluctuate to zero, this simple interpretation of L_K is no longer valid. However, the circuit of Fig. 1(a) can still be used to describe the variation of the whisker impedance. It is also the equivalent circuit usually used to describe the dc resistive transition, where reactive effects vanish. Alternatively, one can describe the impedance variation in terms of an admittance $Y = Z^{-1}$ as indicated in Fig. 1(b). This representation is convenient for comparison with theories which calculate the conductivity. Either of these circuits can clearly represent any form of impedance variation.

As T is increased toward T_c, L_K first begins to deviate from the mean-field value, then, just below T_c, R_F rises very rapidly. The rise of R_F provides the dc resistive transition, which has been studied most extensively by Lukens *et al.*[6] (LWW) and Newbower *et al.*[7] (NBT). Above T_c, Z approaches R_N, and the parameters of Fig. 1(a) are perhaps not the most relevant for discussing the impedance. However, R_F^{-1} is essentially the "excess conductance" studied by numerous authors above T_c.[11]

To explain the observed dc resistive transitions in one-dimensional samples, a model was developed by LA[12] in which R_F is produced below T_c by thermally activated phase slips of 2π in the order parameter ψ. They calculated the free-energy barrier height $\Delta F(T)$ over which the system must pass during a phase slip, and they predicted a transition rate

$$\Gamma(T) = \Omega\, e^{-\Delta F(T)/k_B T}\ , \tag{2}$$

where Ω is an attempt frequency, which they merely estimated. The presence of a current makes the barrier for current increasing slips slightly higher than for current decreasing ones, resulting in a time-averaged voltage

$$V(T) = \Phi_0\Omega\, e^{-\Delta F_0(T)/k_B T}\sinh(I_S/2I_1). \tag{3}$$

Here I_S is the supercurrent, Φ_0 is the flux quantum, and $I_1 = k_B T_c/\Phi_0 = 2.5\times10^{-8}$ A. The average barrier height ΔF_0 varies as $\sigma(T_c - T)^{3/2}$, leading to an exponential drop of resistance with decreasing temperature. The σ dependence implies that this rapid fall of R_F occurs further below T_c for smaller whiskers. Subsequently, MH[13] calculated the prefactor Ω and found it to be considerably smaller than the LA estimate and dependent upon both current and temperature. As LWW and NBT have shown, the combined LA-MH theory can be made to correspond quite well with the lower part of the dc resistive transitions of whiskers if T_c and σ are used as adjustable parameters. However, LWW have suggested that the MH value of Ω may still be too high.

The calculation of MH to obtain the attempt frequency Ω also produced a result for the average supercurrent I_S as a function of the phase gradient of the order parameter along the wire. This result is in fact a calculation of L_K, since $I_S L_K = \Phi_0\Delta\phi/2\pi$, where $\Delta\phi$ is the phase difference between the two ends of the whisker. Their result can be expressed as

$$L_K^{-1} = \frac{2\sigma}{\mu_0 l\lambda_L^2(0)}\left(\frac{T_c - T}{T_c}\right) - \frac{6\pi^2(2)^{1/2}k_B T_c\xi(0)}{\Phi_0^2 l}\left(\frac{T_c}{T_c - T}\right)^{1/2}. \tag{4}$$

We have used the clean-limit result to write $\lambda^2(T) = \lambda_L^2(0)\, T_c/2(T_c - T)$, which defines $\lambda_L(0)$, the zero-temperature London penetration depth. We also write the temperature-dependent coherence length as $\xi(T) = \xi(0)\,[T_c/(T_c - T)]^{1/2}$. Both of these limiting forms for the temperature dependence are valid in the local regime near T_c where our measurements are made.[20] In addition, we assume $I_S \ll I_c$, where I_c is the mean-field critical current. Recalling that $L_K^{-1} \propto \langle|\psi|^2\rangle$, we see that the first term in Eq. (4) is the mean-field result, showing a linear drop of $\langle|\psi|^2\rangle$ to zero at T_c. The second term is a fluctuation suppression of the order parameter below the mean-field line, which in Eq. (4) actually brings $\langle|\psi|^2\rangle$ to zero at a temperature below T_c. However, the whole LA-MH approach assumes that there exists a well-established order parameter. If the fluctuation suppression becomes comparable to $\langle|\psi|^2\rangle$ itself, this assumption is invalid, and a different approach is needed. Thus, the LA-MH theory is expected to break down some distance below T_c.

The only calculation of which we are aware that attempts to describe the fluctuation effects in the ac conductivity of a superconductor all the way through T_c is that of Schmidt.[21] This calculation

is based on a simple time-dependent Ginzburg–Landau theory, and it has had success in describing data on two-dimensional films with short mean-free paths.[22] However, in the dc limit, the Schmidt calculation above T_c leads to the same result as the microscopic calculation of Aslamazov and Larkin.[23] This result disagrees with data on the dc conductivity of clean systems above T_c,[8] even though it does adequately fit dc data on dirty or amorphous films.[24] Thus, it is already clear that the Schmidt calculation should not be expected to describe adequately our ac-conductivity results on these clean whiskers. Indeed it does not, and the nature of the disagreement is documented in Sec. IV.

Two attempts have been made to calculate the dc conductivity through the transition region; that by Masker, Marcelja, and Parks[25] (MMP) and that by Londergan and Langer[26] (LL). The latter calculation attempts only to set an upper limit on the resistance. These are compared with our low-frequency resistance results in Sec. IV.

Scalapino, Sears, and Ferrell[14] and also Grunberg and Gunther[15] have calculated an expression for $\langle|\psi|^2\rangle$ itself through the transition region. Their results agree with the MH result in the region where the latter is valid. Unfortunately, above that region in temperature, the relationship between $\langle|\psi|^2\rangle$ and the impedance is not clear. Since these calculations do not yield the conductivity, we cannot compare our data quantitatively with them.

III. EXPERIMENTAL DESIGN AND TECHNIQUES

The tin whiskers for this study were grown by the "squeeze" method.[27] A stack of stainless-steel washers, every other one coated on one side with approximately 0.3 μm of Sn, was compressed by means of a stainless-steel nut and bolt. The Sn coating was evaporated onto the washers using starting material of nominal 99.999% purity. The evaporation took place in about 5 sec at a pressure of 10^{-7} torr. After the nut was tightened, the outside diameter of the washer stack was turned down in a lathe to produce a smooth growth surface and to keep the Sn layers under pressure out to the edge of the cracks between washers. Growth was accelerated by heating the finished assemblies to 120 °C in a vacuum oven. Whiskers 1–5 mm in length and 0.1–1 μm in diameter were produced in about 3 days at this temperature.

Whiskers were picked from the bolts by hand using tweezers under a stereomicroscope. A whisker of acceptable length, apparent diameter, and growth direction was chosen and sheared off at the base with the tweezer tip to avoid damage to most of its length. The growth direction is an indication of crystal orientation as indicated below. While still in the tweezers, the stiffness, recovery from bending, and smoothness of line of the whisker was examined. If acceptable, the whisker was laid across the four contact wires of the sample holder. After being laid out, whiskers were examined under a high-power optical microscope for evidence of surface flaws or shape differing radically from a circle such as flat or dumbbell shaped cross sections. Only whiskers which appeared generally round and had at most one or two extremely localized features along their lengths at the limits of resolution of the microscope were accepted for further measurements.

The sample holder[28] consisted of four gold contact wires 0.075 mm in diameter glued to a Tedlar[29] film, which could be stretched by means of a differential screw. These wires were quite short and were attached to the center conductors of four 50-Ω coaxial cables leading out of the cryostat. A pair of these formed a 100-Ω balanced transmission line. A whisker laid across and attached to these wires could be strained by stretching the plastic film, and the corresponding changes in resistance and T_c could be measured. From these data, the crystal orientation could be determined unambiguously, using the data of Davis *et al.*[30] and Skove.[31]

Contacts, both electrical and mechanical, were made by evaporating Pb to a depth of 2–3 whisker diameters over the points where the whisker crossed the contact wires. It was usually necessary to break through the oxide layer on a whisker by momentarily applying ~30 V to each pair of leads. A current-limiting resistance was used in series to prevent melting the whisker. High-resistance contacts could also be improved after a whisker was superconducting by successive application of this voltage with progressively lower series resistors. Contact resistances measuring 1–2 Ω were common, and many contacts were apparently superconducting. However, the exact position under the Pb film of a contact resulting from this procedure was uncertain, leading to an uncertainty in the electrical length l of the whisker of about ± 9%.

The resistance of each whisker was measured at room temperature to be used in determining the cross-sectional area to length ratio σ/l after the crystal orientation was known. We used the results of Burckbuchler and Reynolds[32] for the room-temperature electrical resistivity of pure Sn as a function of current direction relative to the tetrad axis. The ratio of room-temperature resistance to normal resistance at 4 K ranged from 100 for the smaller whiskers to 300 for the larger ones.

Following a suggestion by Skove,[31] it was found that whiskers growing along a given crystal axis could be selected visually with few errors. It is

as if all whiskers grow from the cracks between washers with the Sn tetrad axis perpendicular to the plane of the crack. Thus, the angle at which a whisker emerges in an indication of the orientation of its axis relative to the tetrad axis. Whiskers growing along the ⟨001⟩ crystalline direction emerged parallel to the surface of the washer stack. These were easiest to pick up, and they could also be selected with the greatest precision. The bulk of the data presented in this paper is from ⟨001⟩ whiskers.

Whisker impedance was measured using a four-wire technique in which the current input leads and voltage sampling leads are balanced transmission lines as described above. These lines were brought out of the cryostat, and they could be used as four independent leads for dc measurements or matched to unbalanced coaxial lines using transformers. The measuring circuit can be described as follows: Current is delivered to a whisker with temperature-dependent impedance $Z_W(T)$ from a source that presents a known impedance Z_S to the whisker. The detector, which presents a known impedance Z_D to the whisker, measures the voltage across $Z_W(T)$. An effective impedance Z_p was also added in series with $Z_W(T)$ to take account of pickup. For the 60-MHz measurements, the detector was a heterodyne lock-in amplifier developed especially for this work. It measures two output-voltage components in accurate quadrature, and the phase drift is about 0.2° over the course of a data run. This system has been described in detail elsewhere.[33] For 1-kHz measurements, a commercial lock-in amplifier was used, and a commercial nanovoltmeter was used for dc measurements.

In the case of the 60-MHz system, it was necessary to make an accurate calibration of Z_D and Z_S. At lower frequencies these were set high enough to be neglected. The value of Z_S was set by careful matching to within a few percent, while the value of Z_D was determined by substituting known impedance for Z_W. The value of Z_D could then be extracted from the corresponding outputs from the detector with an uncertainty of about 5%. It is also necessary to calibrate the over-all system gain and phase shift. These were determined by comparing the detector output when the whisker is normal, when $Z_W = R_N + j\omega L_M$, with that when the whisker is purely reactive far below T_c. Using the value of R_N determined from a dc measurement the value of $Z(T) = Z_W(T) - j\omega L_M$ can be extracted from the corresponding detector outputs at intermediate temperatures. Typically, points 60 mK above and 140 mK below T_c were chosen for gain calibration. At the lower temperature, L_K was typically 10% or less of L_M, which allowed an estimated value of L_K to be used for calibration purposes.

The experiment was performed inside a screened room constructed of two layers of copper wire mesh. A double μ-metal shield surrounded the Dewar. In addition, the 60-MHz circuit was completely enclosed in an elaborate shield[33] with all input and output leads filtered. The sample holder was enclosed in a He-gas-filled copper can, which was itself suspended in vacuum and connected by a weak thermal link to the helium bath.

Temperature was measured with a low-frequency ac bridge and a Ge resistance thermometer. An error signal from the bridge controlled a heater on the sample can to regulate its temperature. As determined by monitoring the resistance of a whisker near T_c, the short-term temperature stability was ~2 μK, and long-term drifts were ~50 μK/h. The absolute temperature scale set by calibrating the thermometer against the vapor pressure is probably not more accurate than ±5 mK, but relative temperatures are repeatable to ~100 μK.

IV. EXPERIMENTAL RESULTS

This section is divided into three parts. The first presents measurements of mean-field properties of the whiskers, and the latter two describe our data on fluctuation effects in the 60-MHz impedance and in the 1-kHz resistance, respectively.

Mean-Field Properties

Figure 2 shows the behavior of the inverse kinetic inductance L_K^{-1} of a typical whisker as a function of temperature over a fairly broad range below T_c. The values of L_K were extracted from the measured whisker impedance $Z(T)$ using the equivalent circuit of Fig. 1(a). This is the mean-field region, where fluctuations are not important, and L_K^{-1} is directly proportional to the square of the order parameter. If fluctuations are ignored, this quantity rises linearly from zero at T_c and then gradually levels out, becoming constant at much lower temperature. The deviation from linearity is just barely visible on the low-temperature side of Fig. 2, as are the fluctuation effects at T_c. The mean-field line in Fig. 2 has been set by fitting the data over a range $0.2 < L_K^{-1} < 0.8$ nH^{-1}. Error bars on several points indicate our best estimate of the systematic errors involved in determining L_K^{-1} from the data. They reflect mainly calibration uncertainty due to possible phase drift in the 60-MHz lock-in system over the time required to complete a data run, and uncertainty in the value of R_N. The result is an uncertainty in the over-all gain of the system. The intercept fixes T_c within about 0.1 mK, and the slope of the line is determined to about ±5%.

The slope of the mean-field line may be expressed in a number of ways for comparison with other data. In the range where the line is fitted,

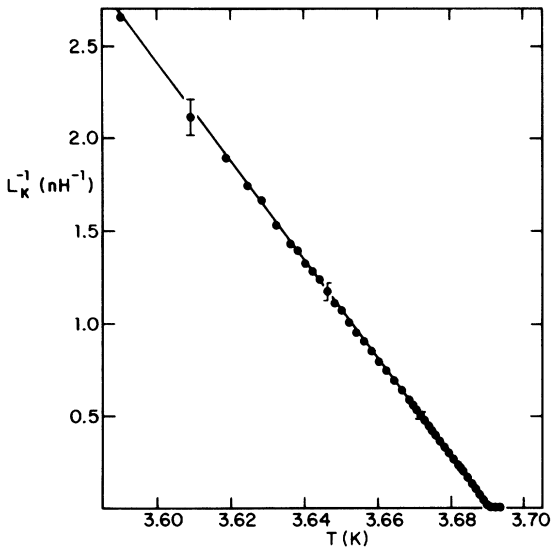

FIG. 2. Mean-field behavior of the inverse kinetic inductance L_K^{-1} of a whisker extracted from $Z(T)$ data measured at 60 MHz using the model of Fig. 1(a). This quantity is proportional to $\langle|\psi|^2\rangle$. The intercept yields T_c, while the slope yields the penetration depth. The mean-field line shown was fitted for $0.2 < L_K^{-1} < 0.8$ nH^{-1}. Fluctuation effects are just visable at T_c, as is the expected departure from linearity on the low-temperature side of the graph.

the penetration depth λ is larger than the whisker diameter. Thus the current is uniform across the whisker. The electrodynamics is local in this range also, and we can interpret L_K in terms of λ; $L_K = \mu_0\lambda^2\sigma/l$. The ratio σ/l of a whisker is determined from its room-temperature resistance and crystal orientation. We have chosen to relate the initial-temperature derivative of λ^{-2} in the mean-field region to the zero-temperature London penetration depth $\lambda_L(0)$ using the BCS result for the limit $T \to T_c$; $\lambda^{-2}(T) = 2\lambda_L^{-2}(0)\,(T_c - T)/T_c$.[20] This provides a value of $\lambda_L(0)$ for comparison with the results of different kinds of measurements. For the whisker shown in Fig. 2, we obtain $\lambda_L(0) = 348 \pm 10$ Å.

Figure 3 shows values of $\lambda_L(0)$ obtained from a number of whiskers oriented along the $\langle 001\rangle$ axis. These are plotted as a function of whisker size. We use $\sigma^{1/2}$ as a size parameter, because only the cross-sectional area of a whisker is determined, not its shape. It is clear that $\lambda_L(0)$ increases as the whisker size decreases. An increase of penetration depth with decreasing mean-free path δ is well known, and Goodman[34] has given a formula to describe this effect. For our purposes it can be written

$$\lambda_L(0) = \lambda_{LP}(1 + 0.752\,\xi_0/\delta)^{1/2}, \qquad (5)$$

where λ_{LP} is the London penetration depth of the "pure" bulk material with $\delta \gg \xi_0$, and ξ_0 is its coherence length. We take $\xi_0 = 2980$ Å.[35] However, the values of δ determined for our whiskers from their residual resistance ratios are too large to explain the size effect shown in Fig. 3, and a plot of $\lambda_L(0)$ against δ determined in this way shows much more scatter than Fig. 3. The curves shown were calculated from Eq. (5) by assuming that the effective mean-free path for determining λ is simply proportional to $\sigma^{1/2}$, i.e., $\delta = f\sigma^{1/2}$. The values of the constants f and λ_{LP} were adjusted to fit the data. The solid curve represents $f = 2.3$ and $\lambda_{LP} = 289$ Å. The other curves indicate the effects of varying these parameters; they represent $f = 1.4$, $\lambda_{LP} = 272$ Å and $f = 4.1$, $\lambda_{LP} = 303$ Å.

The mean-free paths determined from residual-resistance ratios, on the other hand, were typically considerably longer than twice the whisker size; particularly in $\langle 001\rangle$ whiskers. Values of δ determined in this way for whiskers in Fig. 3 ranged from 4 to 7 times $\sigma^{1/2}$. There is obviously considerable specular reflection of quasiparticles at the surfaces of these whiskers. The few whiskers we have measured with growth directions inclined to the tetrad axis, i.e., $\langle 101\rangle$ and $\langle 111\rangle$, showed values of residual resistance more consistent with $\delta \approx 2\sigma^{1/2}$. Evidently, the surfaces of whiskers with these orientations tend to be less perfect.

The discrepancy between the mean-free path indicated by the size dependence of the penetration depth and that determined from the dc conductivity in the normal state indicates to us that the mean-free path in these whiskers is quite anisotropic, perhaps partially due to a dependence of the specular reflection on angle of incidence. Thus, the

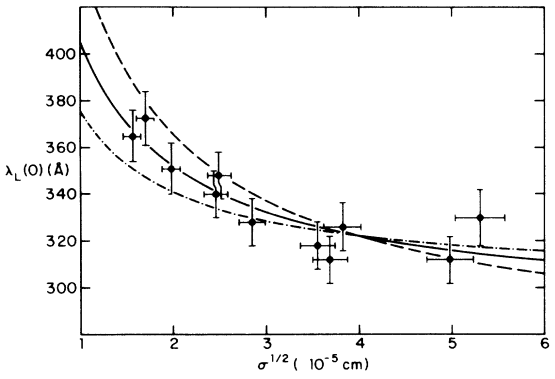

FIG. 3. Values of the zero-temperature London-penetration depth, obtained from mean-field slopes as in Fig. 2 for a number of $\langle 001\rangle$ whiskers and plotted as a function of $\sigma^{1/2}$, where σ is the cross-sectional area. The curves were calculated from the Goodman formula, assuming that the free path is proportional to $\sigma^{1/2}$. See text for the parameters of the curves and a discussion of this procedure.

particular average over the Fermi surface involved in determining λ could be different from that which determines the normal conductivity.

The value of λ_{LP} for tin which is implied by the fit in Fig. 3, namely, $\lambda_{LP} = 289 \pm 20$ Å, is considerably lower than the value which has long been accepted[36] for Sn, namely, $\lambda_{LP} = 355$ Å. However, there have been several experimental indications recently that a lower value is more appropriate. Halbritter[37] found that a value of 280 Å was most consistent with the surface impedance measured at microwave frequencies. Tai *et al.*[38] inferred a value of 290 Å from magnetic measurements of the temperature derivative of λ in a bulk single crystal oriented so that the shielding current flowed in the $\langle 001 \rangle$ direction. This is the direction the measuring current flows in an $\langle 001 \rangle$ whisker such as those in Fig. 3, and our results lend additional support for a lower value of λ_{LP} for Sn.

Fluctuation Effects in the 60-MHz Impedance

Figure 4 shows the region of temperature in which fluctuation effects are important. This is a plot of L_K^{-1} versus temperature for the same whisker represented in Fig. 2, but the scale has been expanded to show the immediate neighborhood of T_c. The solid line is the mean-field line from Fig. 2, obtained from a linear fit to the L_K^{-1} data further down in temperature. As the temperature is increased, the values of L_K^{-1} first fall below the mean-field line, then cross it, and gradually go to zero above T_c.

The dashed curve in Fig. 4 represents the first fluctuation correction to L_K^{-1} as calculated by MH in the form of a current-phase relation. Their result for L_K^{-1} in the zero-current limit is given above in Eq. (4), which was used to calculate the curve. The intercept of the mean-field line has been adjusted slightly in Fig. 4 from the value obtained in Fig. 2 to optimize the fit of the MH curve to the data. The amount of the shift is less than 0.1 mK, which is within the limits allowed by the mean-field fit in Fig. 2.

As discussed in Sec. II, the MH theory is only valid in the region below T_c where the order parameter is well established and the fluctuations are relatively small. Thus, it is not surprising that the data in Fig. 4 leave the MH curve about 1.6 mK below T_c. The point where the data leave the curve is just the point where the dissipation represented by R_F in Fig. 1(a) is becoming comparable to ωL_K. This is the point where the simple interpretation of L_K in terms of $\langle |\psi|^2 \rangle$ breaks down. It is typical of all our whiskers that the values of L_K^{-1} leave the MH curve about 2.1 times as far below T_c as the point where the MH curve intersects the axis. At lower temperatures, the fit is quite good, although there is typically a

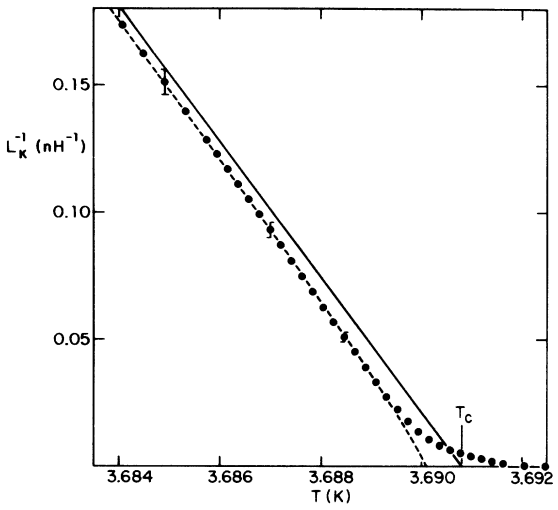

FIG. 4. Values of L_K^{-1} for the same whisker as in Fig. 2 plotted on an expanded scale to show the fluctuation region. The solid line is the mean-field line from Fig. 2, and the dashed curve is the MH prediction for the initial fluctuation suppression of $\langle |\psi|^2 \rangle$ below its mean-field value.

slight deviation of the data below the MH curve as is seen in Fig. 4. This slight suppression of $\langle |\psi|^2 \rangle$ may be due to the finite measuring current (0.2-μA rms), which was not taken into account in calculating the curve.

The calculations mentioned in Sec. II of the behavior of $\langle |\psi|^2 \rangle$ through T_c[14,15] agree with the MH result in the region where the MH curve fits our data. Above the temperature where our data depart from the MH curve, these calculations predict a temperature dependence of $\langle |\psi|^2 \rangle$, which is qualitatively similar to the behavior of L_K^{-1}. It crosses the mean-field line and tails off slowly above T_c. Quantitative agreement is lacking, however, since L_K^{-1} no longer measures $\langle |\psi|^2 \rangle$.

It is not clear what is the best way to present the data for the complete $Z(T)$ as T is raised through T_c. We have chosen simply to present the real and imaginary parts of the admittance of the whisker, $Y_1 + jY_2 = Z^{-1}(T)$, as in Fig 1(b). Note, however, that the magnetic reactance $j\omega L_M$ has been subtracted from the total whisker impedance before the reciprocal is taken. In Fig. 5 are shown the data for "excess" conductance $Y_1 - R_N^{-1}$ and inverse effective shunt inductance $-\omega Y_2$ for the same whisker as in Figs. 2 and 4. We emphasize that the admittance values in Fig. 5 are calculated from the same values of $Z(T)$ as the inductance values in Fig. 4. For $T_c - T > 3$ mK, where Y_1 is essentially R_N^{-1}, $-\omega Y_2$ is essentially equivalent to L_K^{-1}. This is not true above this temperature, as a comparison of Figs. 4 and 5 will

indicate. The mean-field line is shown in Fig. 5 for comparison, and the dashed curve is merely to guide the eye. It has no theoretical basis. Once again the error bars indicate our best estimates of the systematic errors involved in the measurement.

As we have indicated in Sec. II, no attempt beyond that of Schmidt[21] has yet been made to calculate the full ac conductivity in the fluctuation region. The Schmidt calculation fails in several qualitative respects to describe our data. As T is raised toward T_c, it predicts for $-\omega Y_2$ on enhancement above rather than a suppression below the mean-field line, and it predicts a singularity that is not observed in this quantity at T_c. In the case of Y_1, the peak is predicted to occur at T_c. The peak in Y_1 shown in Fig. 5 occurs 1.6 mK below T_c, and is much wider and higher than is predicted.

To facilitate comparison with future calculations, we present in detail the results from one whisker and describe in general the observed variations with whisker size. A detailed profile of one whisker is given in Figs. 2 and 4–6. This whisker is oriented in the ⟨001⟩ direction, its length is $(8.3 \pm 0.7)\times 10^{-2}$ cm, and it has a room-temperature resistance of 2080 Ω. From the room-temperature resistivity of Sn for current in the ⟨001⟩ direction, [32] we calculate the ratio $\sigma/l = 7.45\times 10^{-9}$ cm, and then $\sigma = (6.18 \pm 0.5)\times 10^{-10}$ cm^2. The value of R_N well above T_c was 20.7 Ω, indicating a mean-free path $\delta = 9400$ Å. In addition to this whisker, we have measured the impedance of ⟨001⟩ whiskers ranging in area from 2.4 to 28×10^{-10} cm^2, as indicated in Fig. 3. The position of the peak in Y_1 varies strongly with whisker size, falling 0.8 mK below T_c for the largest whisker measured and 30 mK below T_c for the smallest. The width of the peak, however, depends only weakly on size, varying from 1.6 to 2.0 mK. The ratio of the maximum excess conductance $Y_1 - R_N^{-1}$ to the normal conductance R_N^{-1} varies from about 1.4 for the smallest whisker to 0.14 for the largest.

1-kHz Resistance

At 1 kHz the reactances are negligible, and the resistance data should be equivalent to dc-resistance data. This is true provided that the variation of the resistance with current during a cycle of the ac is properly taken into account.

Resistance data obtained at 1 kHz for three whiskers are shown in Fig. 6. The same data are presented twice, in Figs. 6(a) and 6(b), to facilitate comparison with different theoretical curves discussed below. The normalized resistance of the whiskers is plotted versus $T - T_c$. In terms of the equivalent circuit of Fig. 1(a), this resistance is the parallel combination of R_F and R_N normalized by R_N. For each whisker, the value of T_c was determined from the 60-MHz impedance data using a plot such as Fig. 4. The squares are data from the same whisker represented in Figs. 2, 4, and 5, while the circles and triangles represent whiskers at the small ($\sigma = 2.4 \times 10^{-10}$ cm^2) and large ($\sigma = 25\times 10^{-10}$ cm^2) extremes respectively of our size range. All are ⟨001⟩ whiskers. The measuring current in each case was 0.1-μA rms, which is comparable to the parameter I_1 of the LA-MH theory. At this current level, the nonlinearity of the LA-MH voltage (3) is not too severe, and the effective ac resistance to be expected is easily calculated. The

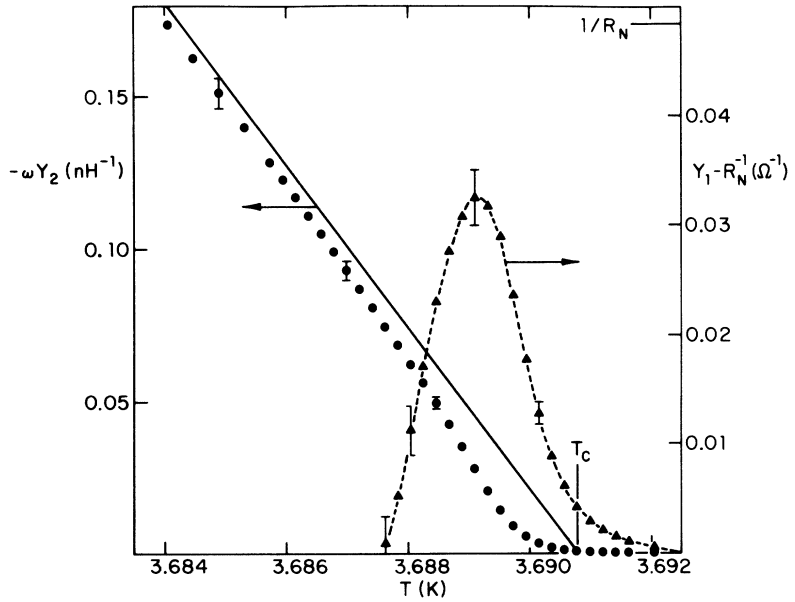

FIG. 5. Full complex admittance $1/Z(T)$ at 60 MHz for the same whisker as in Figs. 2 and 4. (See text for whisker parameters.) The circles are $-\omega Y_2$, which is equivalent to L_K^{-1} only if $R_F = 0$ in the circuit of Fig. 1(a). The mean-field line from Fig. 2 is shown for comparison. Triangles represent the "excess" real conductance $Y_1 - R_N^{-1}$. The dashed curve is merely drawn through the points to guide the eye. It has no theoretical significance.

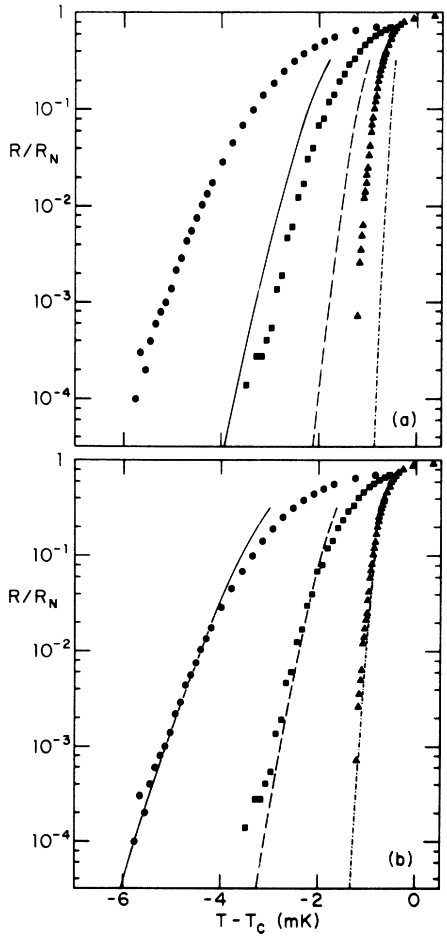

FIG. 6. Resistive transitions for three whiskers measured at 1 kHz. The data are presented twice for comparison with two sets of theoretical curves. The squares represent the same whisker as in Figs. 2, 4, and 5, which has a cross-sectional area $\sigma = 6.2 \times 10^{-10}$ cm^2. Circles and triangles represent whiskers with $\sigma = 2.4 \times 10^{-10}$ and 25×10^{-10} cm^2, respectively. The curves in (a) are the LA-MH predictions using the whisker parameters determined as described in the text. No adjustable parameters are available. The curves in (b) show the effect of reducing the barrier height in the theory of LA by a factor of 0.55 for all three whiskers, leaving its temperature and area dependence unchanged along with the MH prefactor.

curves in Fig. 6(a) are the predictions of LA-MH for each whisker. Values of T_c and σ which enter the LA-MH calculation were obtained as described above. The other material parameter to which the calculated resistance is sensitive is the coherence length $\xi(T)$. In Fig. 6 we have used the clean limit formula[20] for $\xi(T)$ with $\xi_0 = 2980$ Å. This value is consistent with $\lambda_L = 290$ Å and the most recent values[35] of κ, the Ginzburg-Landau parameter. This value was used also by NBT. Taking the clean limit result for ξ is justified if the mean-free path δ is taken from the resistivity ratio data. This was done by NBT and LWW and is done here for comparison with their results. If we take $\delta = 2.3\sigma^{1/2}$, as inferred from Fig. 3, and use Goodman's[34] formula

$$\xi(T) = 0.74\xi_0[1 + 0.75(\xi_0/\delta)]^{-1/2}[T_c/\Delta T]^{1/2},$$

then the fit is improved only slightly. For example, the solid curve would be moved approximately 0.6 mK to the left.

The pattern of disagreement shown in Fig. 6(a) between the LA-MH curves and our data is typical of all the whiskers we have measured. The theoretical curve lies above the data for $R/R_N \gtrsim 0.5$ but falls below at lower values of R. For $R/R_N > 0.5$ we cannot expect agreement, but we do expect agreement for lower values. The predicted exponential fall of R as the temperature is lowered is clearly evident in Fig. 6, and it has been confirmed down to $R/R_N > 2 \times 10^{-6}$ by the dc measurements of NBT. However, the slopes of the LA-MH curves appear to be too steep for our data, and the curves are too high in temperature. The temperature error increases as the whisker size decreases. Adjustment of whisker parameters within the limits set by our other data does not significantly reduce the discrepancy.

In the experiments of NBT and LWW, T_c was used as a free parameter and σ was adjusted within limits to obtain an acceptable fit for $R/R_N \lesssim 0.5$ to dc-resistance data on Sn whiskers. In addition, LWW reduced the attempt frequency, as represented by the prefactor Ω in Eq. (3), by as much as two orders of magnitude. We also could fit our data by using a combination of these techniques, but it would require exceeding the limits of error on T_c and/or σ.

Before discussing this situation further, the possibility must be considered that these discrepancies are caused by interference or pick-up currents in the whiskers. The effect of excess current in a whisker from pick-up or rf interference would be to shift the apparent transition to lower temperatures, and the shifts would be greater for smaller whiskers. However, we do not believe that this is the explanation for the discrepancies shown in Fig. 6(a). It is difficult to prove the absence of pick-up effects, but several points can be made. While sometimes opening the screen-room door causes a whisker connected to the 1-kHz measuring system to go normal, sometimes it does not. No differences are observed in the 1-kHz transition curves taken with the door closed under these two conditions. This indicates that our shielding is good enough so that the outside interference level can change considerably without affecting the data. Furthermore, the 60-MHz sys-

tem has an elaborate shield[33] independent of the screen room, and no such effects of opening the door are observed in the 60-MHz data. Yet values of R_F extracted from the 60-MHz data agree with the 1-kHz R_F data over the range where accurate 60-MHz R_F measurements can be made. This is limited to the upper two decades or so of the resistive transition by the difficulty of extracting a lower value of R_F accurately from the high 60-MHz reactance. These considerations indicate to us that interference is not the likely cause of the discrepancies in Fig. 6(a).

We believe that our results indicate a definite failure of the LA-MH theory to reproduce quantitatively the onset of resistance in one-dimensional superconductors. It is not obvious from the data just which aspect of the theory to question, but we have found some suggestive indications. We do not question the basic idea that the rise of R_F is caused by thermally activated phase slips. Otherwise, it would be very difficult to understand either the exponential onset of resistance, shown in Fig. 6 and found in dc measurements or the $\sinh(I_S/2I_1)$ current dependence measured by LWW. We could then question either the attempt frequency calculated by MH or the barrier height calculated by LA. Altering the attempt frequency, as did LWW, does not lead to better agreement between the LA-MH curves and our data unless T_c is at the same time reduced beyond our limits of error. Reducing the barrier height, on the other hand, allows us to fit data for whiskers which vary more than an order of magnitude in area without changing T_c or the attempt frequency.

Figure 6(b) shows the result of reducing the barrier height in the LA-MH formula without changing either its temperature or area dependence. To calculate the curves in Fig. 6(b) from Eq. (3), the area σ for each whisker was simply replaced by 0.55σ. The result is that all three curves now fit the respective sets of data for $R/R_N < 0.1$ within the limits we can establish for T_c. These limits are determined primarily by drift in the temperature-control system between the time the 60-MHz data run is begun and the 1-kHz data run is completed. The uncertainty is about ± 50 μK for the largest and smallest whiskers in Fig. 6 and about ± 200 μK for the intermediate whisker. The larger limits for the whisker represented by square points reflect a delay of more than 4 h between the 1-kHz measurements and the 60-MHz measurements presented in Figs. 2, 4, and 5. By using a simple reduction in σ to reduce the barrier height, we also slightly reduce the attempt frequency, but the effect of this on the curves in Fig. 6(b) is negligible compared to the effect of reducing the barrier height. Thus, we can fit our measurements of the onset of resistance in whiskers ranging over an order of magnitude in area by reducing the LA barrier height $\Delta F_0(\sigma, T)$ to $0.55\ \Delta F_0(\sigma, T)$. Note that if we use in the calculation of the barrier height values of $\xi(T)$ calculated using $\delta = 2.3\sigma^{1/2}$, the conclusion is qualitatively the same. However, the reduction factor required to produce an acceptable fit for all three whiskers is approximately 0.65 instead of 0.55.

Further support for our conclusion that the barrier height is the problem comes from a comparison of Figs. 4 and 6(a). We note in Fig. 4 that the MH prediction for L_K^{-1} fits the data very well within about 1.6 mK of T_c. On the other hand we note in Fig. 6(a) the substantial discrepancy for $T_c - T > 1.6$ mK between the resistance data for the same whisker (square points) and the LA-MH prediction (dashed curve). Recall that the LA-MH curve in Fig. 6(a) was calculated using the same whisker parameters as the MH curve in Fig. 4. The suppression of L_K^{-1} below the mean-field value as calculated by MH is not a result of the rare phase slips which cause resistance; rather it is caused by small thermal fluctuations of the order parameter about its mean field configuration. The fluctuations are determined by the shape of the free energy surface in the immediate vicinity of the mean-field configuration, while the barrier height is fixed by the nature of this surface far from the mean-field configuration. Thus the fact that MH agrees with the L_K^{-1} data while LA-MH disagrees with the resistance data indicates a problem with the barrier height.

Neither the calculation of MMP[25] nor that of LL[26] adequately describes our resistance data for $0.1 < R/R_N < 1$. The LL result, which is an upper bound on R, lies well above the data, except in the range $0.2 < R/R_N < 0.5$. In this range it agrees reasonably well. The result of MMP is too high at both the upper and lower ends of the transition and too low in the middle.

Finally, we regret that we are unable to present data on the paraconductivity of these whiskers above T_c. The Pb overlay contacts we used seemed to change resistance slowly with temperature above T_c. A resistive transition in the contacts was usually observed also around 3.8 K. These factors prevented an accurate enough determination of R_N to extract reliable values of the paraconductivity even below the contact transition.

†Research supported by the Office of Naval Research.
*Present address: Braddock, Dunn, and McDonald, Inc., Vienna, Va. 22180.
‡Present address: Develco, Inc., Mountain View, Calif. 94040.
[1] R. D. Parks and R. P. Groff, Phys. Rev. Lett. **18**, 342 (1967).

[2]T. K. Hunt and J. E. Mercereau, Phys. Rev. Lett. **18**, 551 (1967).
[3]W. W. Webb and R. J. Warburton, Phys. Rev. Lett. **20**, 461 (1968).
[4]R. J. Warburton, B. R. Patton, W. W. Webb, and J. W. Wilkins, Physica (Utr.) **55**, 324 (1971).
[5]D. R. Overcash, C. L. Watlington, M. J. Skove, and E. P. Stillwell, Physica (Utr.) **55**, 317 (1971).
[6]J. E. Lukens, R. J. Warburton, and W. W. Webb, Phys. Rev. Lett. **25**, 1180 (1972).
[7]R. S. Newbower, M. R. Beasley, and M. Tinkham, Phys. Rev. B **5**, 864 (1972).
[8]G. A. Thomas and R. D. Parks, Phys. Rev. Lett. **27**, 1276 (1971).
[9]A. F. Mayadas and R. B. Laibowitz, Phys. Rev. Lett. **28**, 156 (1972).
[10]Some measurements of the reactance of one-dimensional superconductors were reported by D. K. Rose, in *Proceedings of the Twelfth International Conference on Low Temperature Physics, Kyoto, 1970*, edited by E. Kauda (Academic Press of Japan, Kyoto, 1971), p. 489.
[11]For a discussion of paraconductivity in one-dimensional superconductors, see Ref. 9 and references therein. See R. A. Craven, G. A. Thomas, and R. D. Parks, Phys. Rev. B **7**, 157 (1973) for a discussion of the two-dimensional case.
[12]J. S. Langer and V. Ambegaokar, Phys. Rev. **164**, 498 (1967).
[13]D. E. McCumber and B. I. Halperin, Phys. Rev. B **1**, 1054 (1970).
[14]D. J. Scalapino, M. Sears, and R. Ferrell, Phys. Rev. B **6**, 3409 (1972).
[15]L. W. Gruenberg and L. Gunther, Phys. Lett. A **38**, 463 (1972).
[16]J. M. Pierce, Bull. Am. Phys. Soc. **15**, 1353 (1970).
[17]J. R. Miller and J. M. Pierce, Bull. Am. Phys. Soc. **17**, 333 (1972).
[18]J. R. Miller and J. M. Pierce, in *Proceedings of the Thirteenth International Conference on Low Temperature Physics, Boulder, 1972* (University of Colorado Associate Press, Boulder, to be published).
[19]W. A. Little, *Proceedings of the Symposium on the Physics of Superconducting Devices*, Charlottesville, Virginia, April, 1967, p. S-1 (unpublished). AD661848 available from National Technical Information Service, Springfield, Va. 22151.
[20]P. G. de Gennes, *Superconductivity of Metals and Alloys* (Benjamin, New York, 1966), p. 225.
[21]H. Schmidt, Z. Phys. 216, 336 (1968); Z. Phys. 232, 443 (1970).
[22]S. L. Lehoczky and C. V. Briscoe, Phys. Rev. B **4**, 3938 (1971).
[23]L. G. Aslamazov and A. I. Larkin, Fiz. Tverd. Tela **4**, 1104 (1968) [Sov. Phys.-Solid State **10**, 875 (1968)].
[24]D. G. Naugle and R. E. Glover, Phys. Lett. A **28**, 110 (1968); Phys. Lett. A **28**, 611 (1969).
[25]W. E. Masker, S. Marcelja, and R. D. Parks, Phys. Rev. **188**, 745 (1969).
[26]R. J. Londergan and J. S. Langer, Phys. Rev. B **5**, 4376 (1972).
[27]R. M. Fisher, L. S. Darken, and G. K. Carrol, Acta Metall. **2**, 368 (1954).
[28]E. P. Stillwell, M. J. Skove, and J. H. Davis, Rev. Sci. Instrum. **39**, 155 (1968).
[29]Polyvinyl fluroide film made by E. I. duPont de Nemours and Co., Inc. Note that Mylar film proved unsuccessful in this application, often producing strain in a whisker even when unstrained itself.
[30]J. H. Davis, M. J. Skove, and E. P. Stillwell, Solid State Commun. **4**, 597 (1966).
[31]M. J. Skove (private communication).
[32]F. V. Burckbuchler and C. A. Reynolds, Phys. Rev. **175**, 550 (1968).
[33]J. R. Miller and J. M. Pierce, Rev. Sci. Instrum. **43**, 1721 (1972).
[34]B. B. Goodman, *Reports on Progress in Physics*, edited by A. C. Strickland (The Institute of Physics and the Physical Society, London, 1966), Vol. XXIX, p. 445.
[35]F. W. Smith, A. Baratoff, and M. Cardona, Phys. Kondens. Mater. **12**, 145 (1970).
[36]J. Bardeen and J. R. Schrieffer, *Progress in Low Temperature Physics*, edited by C. J. Gorter (North-Holland, Amsterdam, 1961), Vol. III, p. 170.
[37]J. Halbritter, Z. Phys. **238**, 466 (1970).
[38]P. C. L. Tai, M. R. Beasley, and M. Tinkham, in Ref. 18.